

A simple, artifact-free, virtual source model

Ole Marius Hoel Rindal*, Alfonso Rodriguez-Molares† and Andreas Austeng*

*Department of Informatics
University of Oslo
Oslo, Norway
Email: omrindal@ifi.uio.no

†Department of Circulation and Medical Imaging
Norwegian University of Science and Technology
Trondheim, Norway

Abstract—Retrospective beamforming is a synthetic technique that, by combination of several converging waves, reduces the number of transmission events without reduction of image quality. However, due to a discontinuity in the conventional spherical virtual source model, an artifact occurs at the focal depth where the virtual sources are located.

We correct the artifact by modifying the spherical model by assuming plane wave propagation in a region around the focal depth. This hybrid model is simpler and lighter than the current accepted solution.

Keywords—Retrospective beamforming, virtual source, coherent compounding

I. INTRODUCTION

Retrospective beamforming (RTB) exploits the flexibility of software beamforming and provides higher image quality compared to conventional beamforming for the same number of transmitted events.

RTB can be implemented intuitively using a spherical virtual source transmit delay model. The spherical model processes the transmitted wave as if it were generated by a virtual source located at the focal point.

However, when the virtual sources lie inside the field of view, an artifact occurs due to a discontinuity in the spherical transmit delay model [1], [2]. Nguyen and Prager [3] solved this problem by introducing a more detailed wave propagation model. However, that approach is cumbersome to implement and CPU intensive.

Here we introduce an alternative solution that is both easier to implement and less resource hungry than [3].

II. THEORY

A. Conventional beamforming

Conventional focused beamforming is done per transmitted scan line. One axial line in the resulting ultrasound image is reconstructed from each transmit,

$$S[z] = \sum_{m=0}^{M-1} w_m y_m[z], \quad (1)$$

where M is the number of elements, y_m is the delayed signal from element m , and w_m is a predefined weight. The delays can be calculated as in [4].

B. Retrospective beamforming

Retrospective beamforming is done using pixel-based beamforming. Channel data are beamformed directly into a grid of pixels. Contrary to conventional scan line based

beamforming, the contribution from each transmit is calculated for every pixel in the image. For a focused transmit the contribution of transmit t to pixel $\vec{p} = [x, z]$ can be calculated as

$$S_t[x, z] = \sum_{m=0}^{M-1} w_m[x, z] y_m[x, z], \quad (2)$$

where S_t is the low quality image created from each individual transmit.

These images can be coherently compounded into an image of higher quality in the overlapping regions, as

$$S_{\text{RTB}}[x, z] = \sum_{t=0}^{T-1} w_t[x, z] S_t[x, z]. \quad (3)$$

where T is the number of transmits and w_t is a predefined transmit weight weighting down the non-insonified areas.

The region before and after the focus overlaps in multiple transmissions, while the region around the transmit focus does not overlap. This yields a higher signal strength in the overlapping region, that must be compensated with the inverse normalized sum of all the transmit weight sets w_t .

The total time delay is given by

$$\tau = \tau_{\text{tx}} + \tau_{\text{rx}}, \quad (4)$$

where τ_{tx} is the transmit delay and

$$\tau_{\text{rx}} = \frac{|\vec{x}_j - \vec{p}|}{c}, \quad (5)$$

is the receive delay between pixel \vec{p} and the receiving element at \vec{x}_j , where c is the reference speed of sound.

The receive delay, τ_{rx} , is independent of the transmit. The transmit delay, τ_{tx} , is what is under study, so we will dig deeper into it.

C. Spherical delay model

Using a simple spherical model [5] the transmit delay is calculated as

$$\hat{\tau}_{\text{tx}} = \frac{1}{c} (|\vec{v}_k - \vec{x}_k| + |\vec{p} - \vec{v}_k|), \quad (6)$$

where \vec{v}_k denotes the location of the virtual source, and \vec{x}_k is the center of the transmitting aperture.

The transmit delay has two terms: the travel time from \vec{x}_k to \vec{v}_k , and the travel time from \vec{v}_k to \vec{p} . If the reconstructed point is in front of the focal point the second term will be negative, and otherwise positive. This scenario is illustrated by Fig. 1.

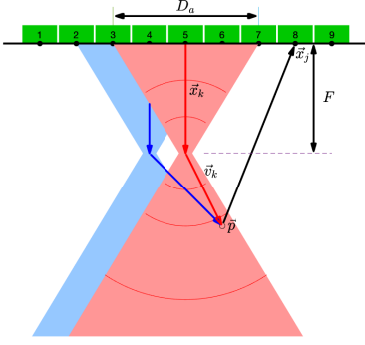


Fig. 1: Delay geometry for a spherical virtual source as depicted in [5]. The blue and red indicate the insonified region from two individual transmits. Notice how they overlap in front of, and after the focal point at F .

By looking at the two terms we can see that at the focal depth, where the second term flips from negative to positive, we will get a discontinuity in the spherical transmit delay model.

D. Unified delay model

In [3] Nguyen and Prager analyzed and divided the transmitted wave field into four regions (I, II, III and IV) as seen in Fig. 2.

Their analysis showed that the transmitted signal is not a single pulse in regions II, and IV, but that it consists of two pulses that are comparable in strength. This violates the spherical wave assumption in regions II and IV, and the spherical transmit delay model is no longer valid.

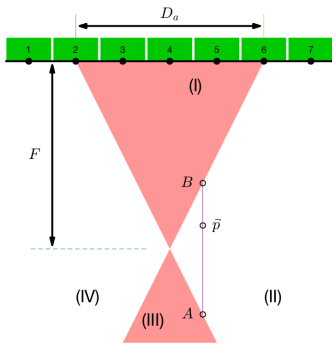


Fig. 2: Delay geometry for the unified transmit delay model as described in [3]. The wavefield is divided into four regions I, II, III and IV. Region I and III follows the spherical model, while the delay for a point \vec{p} in region II and IV is an interpolated value of the delay values in point A and point B.

As regions II and IV are not intensively insonified, the backscattered signal from these regions do not contribute significantly to the total beamformed energy. To correct the

artifact [3] suggested to linearly interpolate the transmit delay between regions I and III, across regions II and IV, and weighting down the amplitude of the data from regions II and IV.

The unified delay model [3] then becomes

$$\hat{\tau}_{\text{tx}} = \frac{|\vec{x}_b - \vec{p}|}{|\vec{x}_b - \vec{x}_a|} \hat{\tau}_{\text{tx},b} + \frac{|\vec{x}_a - \vec{p}|}{|\vec{x}_a - \vec{x}_b|} \hat{\tau}_{\text{tx},a}, \quad (7)$$

where \vec{x}_a and \vec{x}_b are vector positions of points A, B and \vec{p} is the reconstructed point as seen in Fig. 2. $\hat{\tau}_{\text{tx},a}$ and $\hat{\tau}_{\text{tx},b}$ are the delay calculated as in (6) for positions A and B.

E. Hybrid delay model

We present a hybrid transmit delay model combining features of spherical and plane waves. In essence, we assume that the transmit wave propagates as a plane-wave in a small region m around the transmit focus, yielding the transmit delay

$$\tilde{\tau}_{\text{tx}} = \begin{cases} z/c, & \text{if } z > F_z - m \text{ and } z < F_z + m \\ \hat{\tau}_{\text{tx}}, & \text{otherwise.} \end{cases} \quad (8)$$

where F_z is the focal depth.

The three delay models and geometries presented here are valid for linear focused scans. However they can also be derived for sector scans and phased arrays.

III. METHODS

The three models have been implemented for both linear and sector scans in the UltraSound ToolBox (USTB) [6] for both RTB and multiple line acquisition (MLA) reconstruction. The data and code are available through www.ustb.no/examples/hybrid_virtual_source_model.

A RTB sequence was recorded on a Verasonics Vantage 256 system using a Philips L7-4 probe. 128 virtual sources were placed at 29.6 mm depth, ranging from -19 to 19 mm in the lateral direction. A commercial CIRS phantom (Model 054GS) was used as target. The channel data was beamformed with the USTB using 4 MLAs (1 transmit overlap) and full RTB reconstruction with a tukey 25% window on both transmit and receive apodization. A F-number of 2 was used for the transmit apodization, and 1.7 for the receive apodization.

IV. RESULTS

Fig. 3a displays the B-mode image generated using scanline-based beamforming with equation (1). Figs. 3b, 3c and 3d show, respectively, the B-mode image generated with the conventional spherical model, equation (6); with the unified model, equation (7); and the proposed hybrid model, equation (8).

Fig. 4 provides a close up look at the images in Fig. 3. We observe the poorer resolution of scanline-based imaging compared to RTB processing. The improved resolution, together with the reduced sidelobe level of RTB is shown numerically with the lateral profile included in Fig. 5 for a point scatterer at $z=58.5$ mm depth. The close ups highlight also the artifact with the spherical model. Notice that the

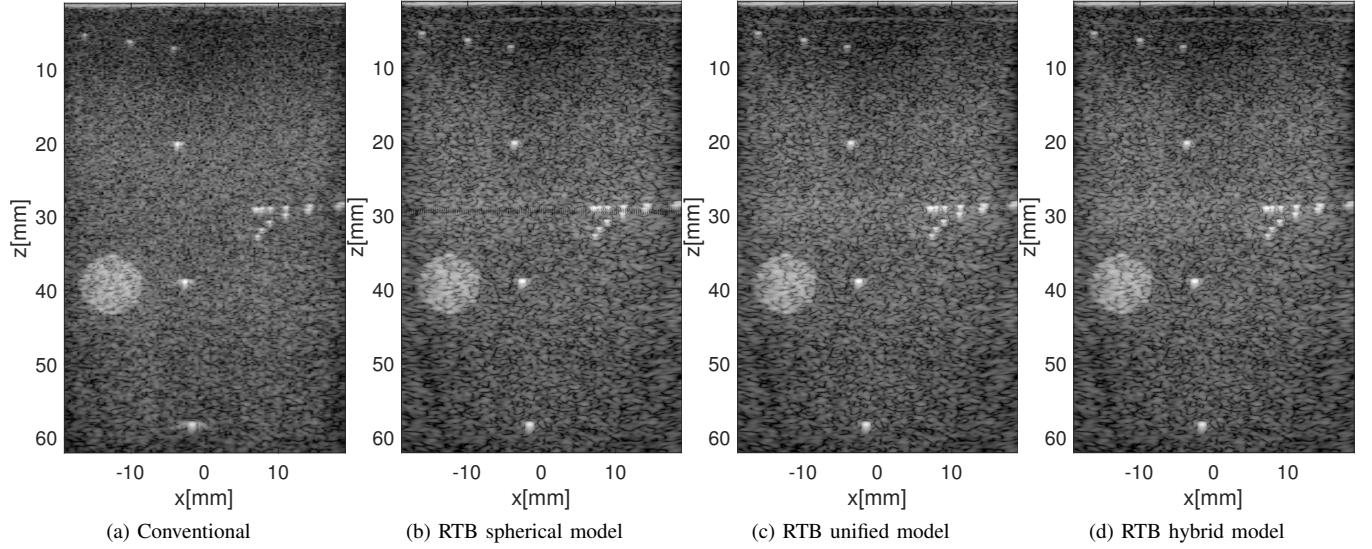
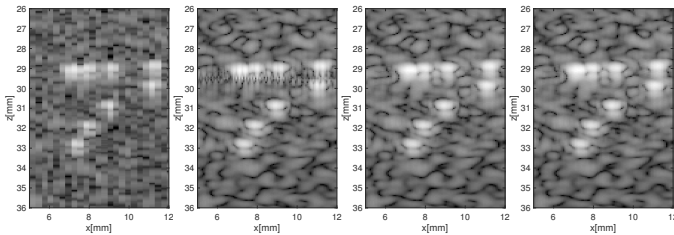


Fig. 3: Images of the CIRS phantom created using conventional beamforming in (a), retrospective beamforming (RTB) with the spherical transmit delay model in (b), RTB with the unified transmit delay model in (c) and RTB with the hybrid transmit delay model in (d). The images are shown with 60 dB dynamic range.

artifact is completely removed using either the unified or the proposed hybrid models.

The calculated delays for all pixels in the field of view are shown in Fig. 6. The aforementioned discontinuity can be observed at 29.6 mm depth in Fig. 6a. The unified model removes the discontinuity completely, Fig. 6b; while the hybrid model pushes it out of the insonified area, Fig. 6c.



(a) Conventional (b) RTB sph. mod. (c) RTB uni. mod. (d) RTB hyb. mod.

Fig. 4: The images in Fig. 3 enhancing the region around the transmit focal depth.

Fig. 7 shows the low quality single transmit images reconstructed with the three models under study without the transmit apodization applied, while Fig. 8 provides a close up of the focal region in Fig. 7 with the transmit apodization applied.

V. DISCUSSION

The artifact, shown at the focal depth (29.6 mm) is visible in the image generated with the conventional spherical model in Fig. 3b and 4b. This artifact originates because of the discontinuity in the delay shown in Fig. 6a. Even though the effect of the discontinuity is small in the low quality images in Fig. 7a and 8a, the effect becomes more apparent by combination of several low quality images, resulting in the artifact observed in the compounded image.

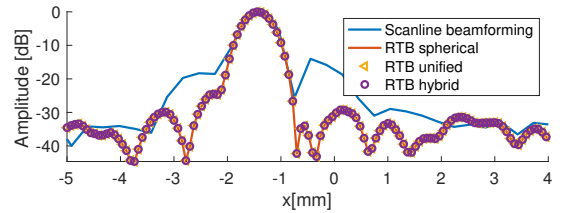


Fig. 5: The lateral line through the wire target at $z = 58.5$ mm.

The unified delay model does not have a discontinuity in the delay model as seen in Fig. 6b. Thus, there is no artifact in the single transmit images Fig. 8b and 7b nor in the final compounded image Fig. 3c and 4c.

The proposed hybrid model does not remove the discontinuity, see Fig. 6c. However, it moves it out of the insonified

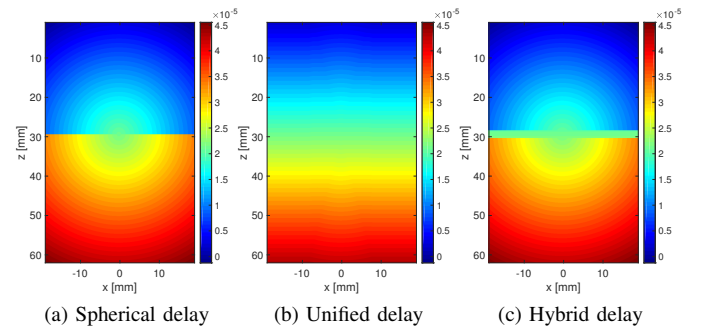


Fig. 6: The transmit delays for the center transmit (64 out of 128) for the spherical model (a), the unified model (b) and the hybrid model (c).

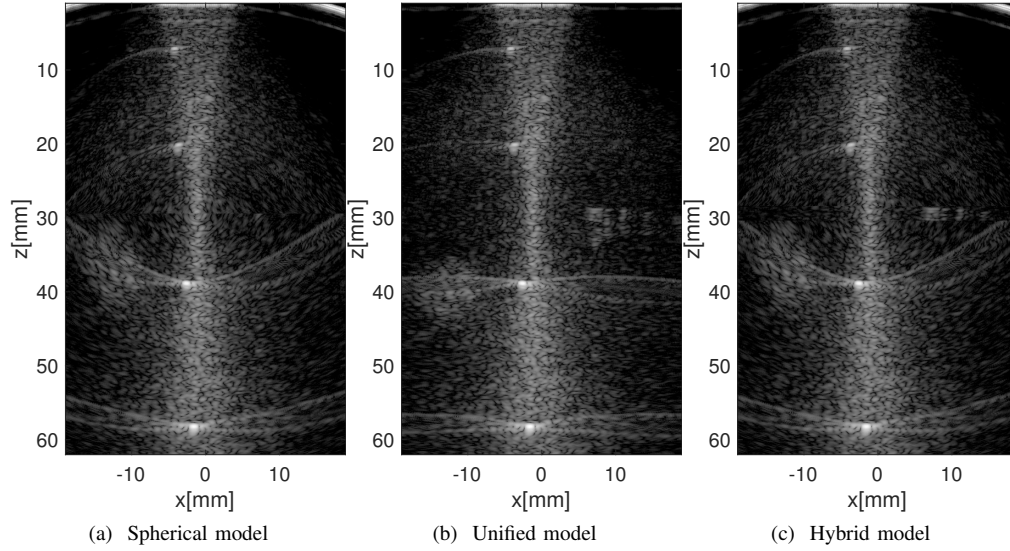


Fig. 7: The full low quality image from a single transmit without transmit apodization for the retrospective beamforming (RTB) with the spherical transmit delay model in (a), the unified transmit delay model in (b) and the hybrid transmit delay model in (c). The images are shown with 60 dB dynamic range.

area, effectively removing the artifact in the final compounded image in Fig. 3d and 4d. This modification does not affect lateral resolution noticeably since focused beams are almost plane at the focal depth.

The artifact is equally removed by both the hybrid and the unified model. However, the hybrid model is easier to implement, and less CPU intensive because it avoids the interpolation operation.

Some interesting differences are observed in the low quality images in Fig. 7: the edge waves produced by the wire targets are more or less straight in the unified model (Fig. 7b) while they are hyperbolic in the spherical (Fig. 7a) and hybrid model

(Fig. 7c). One can also notice a structure in the right hand side of Figs. 7b and 7c, that is not visible in Fig. 7a, presumably coming from a group of scatterers centered at $[x, z] = [10, 30]$ mm.

VI. CONCLUSION

We have introduced a hybrid transmit delay model for retrospective (RTB) beamforming correcting the artifact originating at the focal depth when using the conventional spherical virtual source transmit delay model. The artifact occurs because of a discontinuity in the spherical transmit delay model. This hybrid model consist of a modification to the conventional model by assuming plane-wave propagation in a small region around the transmit focus depth.

REFERENCES

- [1] C. Kim, C. Yoon, J. H. Park, Y. Lee, W. H. Kim, J. M. Chang, B. I. Choi, T. K. Song, and Y. M. Yoo, "Evaluation of ultrasound synthetic aperture imaging using bidirectional pixel-based focusing: Preliminary phantom and in vivo breast study," *IEEE Transactions on Biomedical Engineering*, vol. 60, no. 10, pp. 2716–2724, 2013.
- [2] N. Bottenus, B. C. Byram, J. J. Dahl, and G. E. Trahey, "Synthetic aperture focusing for short-lag spatial coherence imaging," *IEEE Transactions on Ultrasonics, Ferroelectrics, and Frequency Control*, vol. 60, no. 9, pp. 1816–1826, 2013.
- [3] N. Q. Nguyen and R. W. Prager, "High-Resolution Ultrasound Imaging With Unified Pixel-Based Beamforming," *IEEE Trans. Med. Imaging*, vol. 35, no. 1, pp. 98–108, 2016.
- [4] O. T. von Ramm and S. W. Smith, "Beam Steering with Linear Arrays," *IEEE Transaction on Biomedical Engineering*, vol. 30, no. 8, pp. 438–452, 1983.
- [5] S. I. Nikolov, J. Kortbek, and J. A. Jensen, "Practical applications of synthetic aperture imaging," *2010 IEEE International Ultrasonics Symposium*, pp. 350–358, 2010.
- [6] A. Rodriguez-Molares, O. M. H. Rindal, O. Bernard, A. Nair, M. A. L. Bell, H. Liebgott, A. Austeng, and L. Løvstakken, "The UltraSound ToolBox," *Ultrasonics Symposium (IUS), 2017 IEEE International*, pp. 1–4, 2017.

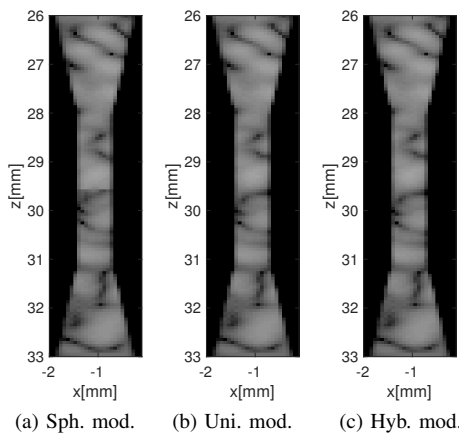


Fig. 8: The images in Fig. 7 but with the transmit apodization applied and enhancing the area around the transmit focal point. Notice the discontinuity at 29.6mm in the image from the spherical transmit delay model (a).